0026-895X/05/6804-1114–1126$20.00
MOLECULAR PHARMACOLOGY
Vol. 68, No. 4
15115/3053746

Mol Pharmacol 68:1114–1126, 2005
Printed in U.S.A.

Characteristics of Ginsenoside Rg_3-Mediated Brain Na^+ Current Inhibition

Jun-Ho Lee, Sang Min Jeong, Jong-Hoon Kim, Byung-Hwan Lee, In-Soo Yoon, Joon-Hee Lee, Sun-Hye Choi, Dong-Hyun Kim, Hyewhon Rhim, Sung Soo Kim, Jai-Il Kim, Choon-Gon Jang, Jin-Ho Song, and Seung-Yeol Nah

Research Laboratory for the Study of Ginseng Signal Transduction and Department of Physiology, College of Veterinary Medicine, Konkuk University, Seoul, Korea (Ju.-H.L., S.M.J., J.-H.K., B.-H.L., I-S.Y., Jo.-H.L., S.-H.C., S.-Y.N); College of Pharmacy, KyungHee University, Seoul, Korea (D.-H.K.); Biomedical Research Center, Korean Institute of Science and Technology, Seoul, Korea (H.R.); Korea Food Research Institute, Gyeonggi-do, Korea (S.S.K.); Department of Life Science, Kwangju Institute of Science & Technology, Kwangju, Korea (J.-I.K.); Department of Pharmacology, College of Pharmacy Sungkyunkwan University, Seoul, Korea (C.-G.J.); and Department of Pharmacology, College of Medicine, Chung-Ang University, Seoul, Korea (J.-H.S.)

Received May 24, 2005; accepted July 13, 2005

ABSTRACT

We demonstrated previously that ginsenoside Rg_3 (Rg_3), an active ingredient of *Panax ginseng*, inhibits brain-type Na^+ channel activity. In this study, we sought to elucidate the molecular mechanisms underlying Rg_3-induced Na^+ channel inhibition. We used the two-microelectrode voltage-clamp technique to investigate the effect of Rg_3 on Na^+ currents (I_{Na}) in *Xenopus laevis* oocytes expressing wild-type rat brain $Na_V1.2$ α and $\beta1$ subunits, or mutants in the channel entrance, the pore region, the lidocaine/tetrodotoxin (TTX) binding sites, the S4 voltage sensor segments of domains I to IV, and the Ile-Phe-Met inactivation cluster. In oocytes expressing wild-type Na^+ channels, Rg_3 induced tonic and use-dependent inhibitions of peak I_{Na}. The Rg_3-induced tonic inhibition of I_{Na} was voltage-dependent, dose-dependent, and reversible, with an IC_{50} value of 32 $\pm$ 6 μM. Rg_3 treatment produced a 11.2 $\pm$ 3.5 mV depolarizing shift in the activation voltage but did not alter the steady-state inactivation voltage. Mutations in the channel entrance, pore region, lidocaine/TTX binding sites, or voltage sensor segments did not affect Rg_3-induced tonic blockade of peak I_{Na}. However, Rg_3 treatment inhibited the peak and plateau I_{Na} in the IFMQ3 mutant, indicating that Rg_3 inhibits both the resting and open states of Na^+ channel. Neutralization of the positive charge at position 859 of voltage sensor segment domain II abolished the Rg_3-induced activation voltage shift and use-dependent inhibition. These results reveal that Rg_3 is a novel Na^+ channel inhibitor capable of acting on the resting and open states of Na^+ channel via interactions with the S4 voltage-sensor segment of domain II.

Na^+ channels are transmembrane proteins that consist of a pore-forming α subunit and auxiliary $\beta1$, $\beta2$, and $\beta3$ subunits (Catterall, 1987; Goldin, 1995; Wang et al., 2003). The α subunit is composed of four homologous domains (I–IV), each composed of six α-helical transmembrane segments (S1–S6). Among them, the S4 segment acts as the voltage-sensing apparatus of the Na^+ channel (Hodgkin and Huxley, 1952). The pore-forming α subunit is responsible for voltage-dependent increases in Na^+-selective permeability. These changes trigger the inward Na^+ current (I_{Na}), which initiates axonal and somatic action potentials in nerve and muscle fibers and may also be involved in axonal information transfer for intraneuronal or interneuronal communications (Hodgkin and Huxley, 1952; Stuart and Sakmann, 1994). Na^+ channels can exist in resting (closed), open (active), or inactivated states and transition among the various states in response to time- and voltage-dependent signaling (Hodgkin and Huxley, 1952). Various drugs can exhibit differential affinities to the specific Na^+ channel states. For example, lidocaine (a local anesthetic) and phenytoin (an anticonvulsant) show a low affinity for the resting state and a higher affinity for the inactivated state, whereas flecainide (an an-

This work was supported in part by a grant from the Korean Food Research Institute (2003), the Neurobiology Research Program from the Korean Ministry of Science and Technology (to S.Y.N.), and two Brain Research Center of the 21st Century Frontier Research Program grants funded by the Korea Ministry of Science and Technology (M103KV010008-05K2201-00830 and M103KV010004-03K2201-00420).

Ju.-H.L. and S.M.J. contributed equally to this work.

Article, publication date, and citation information can be found at http://molpharm.aspetjournals.org.
doi:10.1124/mol.105.015115.

ABBREVIATIONS: Rg_3, 20-*S*-protopanaxadiol-3-[*O*-β-D-glucopyranosyl (1→2)-β-glucopyranoside]; TTX, tetrodotoxin; IFMQ3, Ile1488-Phe1489-Met1490 mutated to I1488Q-F1489Q-M1490Q; DPH, diphenylhydantoin.

tiarrhythmic drug) inhibits the open state (Bean et al., 1983; Hondegham and Kazung, 1984). Na^+ channel modulators that act as drugs and/or neurotoxins often affect both permeation and gating properties (Goldin, 1995), and site-directed mutagenesis studies have allowed characterization of the detailed action and binding sites of various drugs and toxins that regulate neuronal Na^+ channel activity (Catterall, 1987; Goldin, 1995; Wang et al., 2004).

Ginseng, the root of *Panax ginseng* C.A. Meyer, is well known in herbal medicine as a tonic and restorative agent. The main molecular ingredients responsible for the actions of ginseng are the ginsenosides (also called ginseng saponins), which are amphiphilic molecules comprising a hydrophobic backbone of aglycone (a hydrophobic, four-ring, steroid-like structure) linked to hydrophilic carbohydrate side chains consisting of monomers, dimers, or tetramers (Fig. 1). The ginsenosides are classified as protopanaxadiol or protopanaxatriol, according to the positions of the carbohydrate moieties at carbons -3, -6, and -20, which can be either free or connected to sugar rings (Nah, 1997). We recently demonstrated that ginsenoside Rg_3 (20-*S*-protopanaxadiol-3-[*O*-β-D-glucopyranosyl (1→2)-β-glucopyranoside]) (Rg_3), one of the active ingredients in *Panax ginseng*, inhibits voltage-dependent brain Na^+ channel activity expressed in *Xenopus laevis* oocytes (Jeong et al., 2004; Kim et al., 2005). However, no previous work has examined the underlying mechanisms by which Rg_3 regulates Na^+ channel currents.

We herein sought to characterize ginsenoside-mediated Na^+ channel regulation in an *X. laevis* oocyte gene expression system. This model system has few endogenous ion channels (Dascal, 1987) and allows heterologous expression of ion channels for various biochemical studies (Choi et al., 2002, 2003; Sala et al., 2002). We expressed brain Na^+ channels by intraoocyte injection of cRNAs encoding the $Na_V1.2$ α and $\beta1$ subunits (Pugsley and Goldin, 1998; Pugsley et al., 2000) with or without various mutations and examined the changes in I_{Na} in response to Rg_3 treatment. We found that Rg_3 caused both tonic and use-dependent inhibitions of the peak I_{Na} after low- and high-frequency stimulations. We further found that mutations in the channel pore entrance, pore region, lidocaine binding sites, tetrodotoxin (TTX) binding sites, and S4 voltage sensor segments of domains I–IV of the Na^+ channel had no effect on Rg_3-induced tonic inhibition of peak I_{Na}. However, when inactivation cluster Ile1488-Phe1489-Met1490 was mutated to I1488Q-F1489Q-M1490Q (IFMQ3) (West et al., 1992) to create an inactivation-deficient mutant, Rg_3 treatment inhibited both the peak and noninactivating plateau I_{Na} levels of this mutant, indicating that Rg_3 regulates the resting and open states of the expressed Na^+ channel. A single Lys-to-Gln mutation at residue 859 (K859Q) within the S4 voltage sensor segment of domain II abolished the Rg_3-induced shift of the activation voltage and use-dependent inhibition, although changes in the other domains did not. Taken together, these results show for the first time that Rg_3 acts as a novel Na^+ channel blocker by interacting with the S4 voltage-sensor segment of domain II.

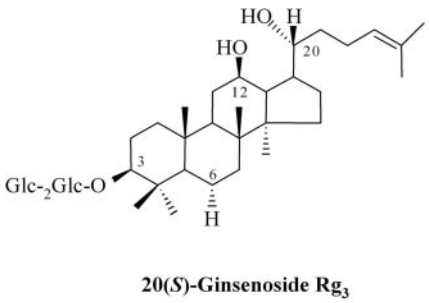

20(*S*)-Ginsenoside Rg_3

Fig. 1. Structure of the 20(*S*)-ginsenoside Rg_3 (Rg_3). Glc, glucopyranoside. Subscripts indicate the carbon in the glucose ring that links the two carbohydrates.

Experimental Procedures

Materials. The 20(*S*)-ginsenoside Rg_3 (Fig. 1) was kindly provided by the Korean Ginseng Cooperation (Taejon, Korea). The cDNA for the rat brain Na^+ channel $Na_V1.2$ α subunit was kindly provided by Dr. A. L. Goldin (University of California, Irvine, CA) and that for the Na^+ channel $\beta1$ subunit was kindly provided by Dr. T. Zimmer (Friedrich Schiller University, Jena, Germany). Other agents were purchased from Sigma (St. Louis, MO).

Preparation of *X. laevis* Oocytes and Microinjection. *X. laevis* frogs were purchased from Xenopus I (Ann Arbor, MI). Their care and handling was in accordance with the highest standards of institutional guidelines. For isolation of oocytes, frogs were anesthetized with an aerated solution of 3-amino benzoic acid ethyl ester, and ovarian follicles were removed. The oocytes were separated by treatment with collagenase and agitation for 2 h in Ca^{2+}-free medium containing 82.5 mM NaCl, 2 mM KCl, 1 mM $MgCl_2$, 5 mM HEPES, 2.5 mM sodium pyruvate, 100 units/ml penicillin, and 100 μg/ml streptomycin. Stage V–VI oocytes were collected and stored in ND96 (96 mM NaCl, 2 mM KCl, 1 mM $MgCl_2$, 1.8 mM $CaCl_2$, and 5 mM HEPES, pH 7.5) supplemented with 0.5 mM theophylline and 50 μg/ml gentamicin. This oocyte-containing solution was maintained at 18°C with continuous gentle shaking and was renewed everyday. Electrophysiological experiments were performed within 5 to 6 days of oocyte isolation, with chemicals applied to the bath. For Na^+ channel experiments, 40 nl of cRNAs encoding the $Na_V1.2$ α and $\beta1$ subunits was injected into the animal or vegetal pole of each oocyte one day after isolation, using a 10-μl VWR microdispenser (VWR Scientific, San Francisco, CA) fitted with a tapered glass pipette tip (15–20 μm in diameter; Choi et al., 2003).

Site-Directed Mutagenesis of $Na_V1.2$ and in Vitro Transcription of Na^+ Channel Subunit cDNAs. The substitution mutations of single or triplet amino acids were performed using the QuikChange XL site-directed mutagenesis kit (Stratagene, La jolla, CA), along with *Pfu* DNA polymerase and mutated sense and antisense primers. Overlap extension of the target domain by sequential polymerase chain reactions was carried out according to the manufacturer's recommended protocol. The final PCR products were transformed to *Escherichia coli* strain DH5α, screened by PCR and confirmed by DNA sequencing of the target region. The mutant DNA constructs were linearized at the 3′ end by NotI digestion, and run-off transcripts were prepared using methylated cap analog $m^7G(5')ppp(5')G$. The cRNAs were prepared using the mMessage mMachine transcription kit (Ambion, Austin, TX) with T7 RNA polymerase. The absence of degraded RNA was determined by denaturing agarose gel electrophoresis followed by ethidium bromide staining. Likewise, recombinant plasmids containing wild-type $Na_V1.2$ α or $\beta1$ subunit cDNA inserts were linearized by digestion with the appropriate restriction enzymes, and cRNAs were obtained using the mMessage mMachine in vitro transcription kit (Ambion) with SP6 RNA or T7 polymerases. The final cRNA products were resuspended at a concentration of 1 μg/μl in RNase-free water and stored at −80°C until use (Choi et al., 2003).

Data Recording. A custom-made Plexiglas net chamber was used for two-electrode voltage-clamp recordings. The chamber was constructed by milling two concentric wells into the chamber bottom

(the diameter and height of the upper well were 8 and 3 mm, respectively, and those of the lower well were 6 and 5 mm, respectively) and gluing plastic meshes (~0.4-mm grid diameter) onto the bottom of the upper well. A perfusion inlet (~1 mm in diameter) was drilled through the wall of the lower well, and a suction tube was placed on the edge of the upper well. For experiments, a single oocyte was placed on the net separating the upper and lower wells. The net grids helped anchor the oocyte in place during the electrophysiological recordings. The oocyte was then impaled with two microelectrodes filled with 3 M KCl (0.2–0.7 MΩ) and electrophysiological experiments were carried out at room temperature using an oocyte clamp (Warner Instruments, Hamden, CT). Stimulation and data acquisition were controlled with a pClamp 8 (Axon Instruments, Union City, CA) (Choi et al., 2003). For most of the electrophysiological experiments on Na^+ channel activity, oocytes were clamped at a holding potential of −100 mV and the membrane potential was depolarized to −10 mV for 100 ms every 5 s. Linear leak currents were corrected by means of the leak subtraction procedure (Jeong et al., 2005).

The voltage-dependence of Na^+ channel activation was calculated by measuring the peak current at test potentials ranging from −50 mV to +50 mV evoked in 5-mV increments. The conductance (g_{Na}) was calculated according to the equation, $g_{Na} = I_{Na}/(V_g - V_r)$, where I_{Na} is the peak amplitude of the Na^+ current, V_g is the test potential, and V_r is the reversal potential for Na^+. The conductance-voltage curves were drawn according to the equation $g_{Na}/g_{Na\ max} = 1/\{1+ \exp[(V_{g0.5} - V_g)/kg]\}$, where $g_{Na\ max}$ is the maximum value for g_{Na}, $V_{g0.5}$ is the potential at which g_{Na} is 0.5 $g_{Na\ max}$, and kg is the slope factor (potential required for an e-fold change). The voltage-dependence of Na^+ channel inactivation was determined using 200 ms conditioning prepulses ranging from −60 mV to +20 mV from a holding potential of −100 mV in 5-mV increments, followed by a test pulse to −10 mV for 5 ms. The peak I_{Na} was normalized to its respective maximum value ($I_{Na\ max}$) and plotted as a function of the prepulse potential. The steady-state inactivation curves were drawn according to the equation $I_{Na}/I_{Na\ max} = 1/\{1 + \exp[(V_h - V_{h0.5})/kh]\}$, where V_h is the prepulse potential, $V_{h0.5}$ is the potential at which I_{Na} is 0.5 $I_{Na\ max}$, and kh is the slope factor.

The frequency-dependent effect of Rg_3 was examined using a protocol in which 50 depolarizing pulses of 10-ms duration and 10 Hz frequency were applied to −10 mV from a holding potential of −100 mV. The protocol was run in the absence (control) and presence of 10 or 100 μM Rg_3. The current amplitude of each pulse was normalized to the peak maximal current (pulse number 1) and plotted as a function of pulse number.

The kinetics of the Rg_3 blockade of IFMQ3, which is the fast-inactivation–deficient mutant of $Na_V1.2$, were examined by clamping oocytes at −100 mV in ND96 solution. A single 500-ms depolarizing pulse to −10 mV was applied, and the I_{Na} was recorded. Different concentrations of Rg_3 (10, 30, 100, or 300 μM) were perfused into the bath for 1 min, and a second, single depolarizing pulse from −100 to −10 mV was given. The data were individually fit to either a single $[1 - A_{slow} \times \exp(-t/\tau_{slow})]$ or double $[1 - A_{fast} \times \exp(-t/\tau_{fast})] + [1 - A_{slow} \times \exp(-t/\tau_{slow})]$ exponential equation, in which A_{fast} and A_{slow} represent the proportion of current decaying with time constants τ_{fast} and τ_{slow}, respectively, and t is the time interval. If we assume that a first-order relationship describes the dependence of the blocking rate on the concentration of the blocking chemical, the apparent rate constant for binding (k_{on}) can be obtained by fitting the τ_{fast} values with the equation: $1/\tau_{fast} = k_{on} \times [Rg_3] + l$ (Lansman et al., 1986). Recovery from open channel blockade was measured at a holding potential of −100 mV with a 10-ms depolarizing prepulse to −10 mV (P1) followed by a variable recovery period from 10 to 500 ms, subsequently followed by a 10-ms test pulse to −10 mV (P2).

Data Analysis. To obtain the concentration-response curve of the effect of Rg_3 on I_{Na}, the peak amplitudes at different concentrations of Rg_3 were plotted and then fitted to the following Hill equation using the Origin software (OriginLab Corp, Northampton, MA): $y/y_{max} = [A]^{nH}/([A]^{nH} + [EC_{50}]^{nH})$, where y is the peak I_{Na} at given concentration of Rg_3, y_{max} is the maximal peak I_{Na}, EC_{50} is the concentration of Rg_3 producing a half-maximum effect, [A] is the concentration of Rg_3, and n_H is the interaction coefficient. All values are presented as means ± S.E.M. The differences between the means of control and treatment values were determined using an unpaired Student's t test. A value of $P < 0.05$ was considered statistically significant.

Results

The Effect of Rg_3 on Peak I_{Na} in Oocytes Expressing $Na_V1.2$. The effect of Rg_3 on currents from brain Na^+ channels expressed in *X. laevis* oocytes was examined. I_{Na} was recorded by two-electrode voltage clamping of oocytes injected with cRNAs encoding $Na_V1.2$ α and β1 subunits. Oocytes were held at −100 mV, and I_{Na} was elicited by depolarization to −10 mV at a low frequency (0.2 Hz). This procedure minimized the use-dependent blockade and allowed evaluation of whether Rg_3 produced a tonic blockade of peak I_{Na} (Pugsley and Goldin, 1998; Pugsley et al., 2000). For comparison, we also examined the effect of lidocaine on the peak I_{Na}. As shown in Fig. 2A, the depolarizing voltage step induced a large inward I_{Na} with rapid inactivation. Application of Rg_3 (100 μM) or lidocaine (1000 μM) inhibited the peak I_{Na} by 64 ± 7 and 41 ± 10%, respectively (Fig. 2A, inset), indicating that both agents induced a tonic inhibition of the Na^+ current.

Concentration-Dependent Inhibition of I_{Na} by Rg_3 or Lidocaine. The current-voltage relationships were assessed in the absence or presence of Rg_3 with voltage steps ranging from −50 to +50 mV evoked from a holding potential of −100 mV every 5 s. As shown in Fig. 2B, addition of Rg_3 caused a voltage-dependent reduction in peak I_{Na}, with a more pronounced reduction noted at lower voltage ranges. In addition, Rg_3 treatment shifted the threshold voltage of channel opening and the voltage of the peak I_{Na} to more depolarized values compared with the control. However, Rg_3 had no significant effect on the kinetics of current decay. As shown in Fig. 2C, the inhibitory effect of Rg_3 on peak I_{Na} was dose-dependent up to 300 μM, with an estimated IC_{50} value of 32 ± 6 μM. The Hill coefficient was 1.1 ± 0.4, indicating that one molecule of Rg_3 seemed sufficient to block one Na^+ channel. We also tested the effect of lidocaine on peak I_{Na} and found that it was dose-dependent up to 3000 μM (Fig. 2C). The IC_{50} was 966 ± 37 μM, which is consistent with previous report (Pugsley and Goldin, 1998). These findings indicate that Rg_3 was more potent than lidocaine by approximately33.2-fold. It is noteworthy that the IC_{50} value for Rg_3-mediated Na^+ current inhibition was 2-fold higher than that for Rg_3-induced inhibition of Na^+ influxes triggered by acetylcholine treatment in bovine adrenal chromaffin cells (Tachikawa et al., 1995) and 8-fold higher than that for Rg_3-induced inhibition in $[Ca^{2+}]_i$ increase by NMDA treatment in rat hippocampal neurons (Kim et al., 2002). These discrepancies in IC_{50} values might reflect the differential affinity of Rg_3 for ion channels or receptors, suggesting that NMDA or nicotinic acetylcholine receptors might be more sensitive than Na^+ channels to low concentrations of Rg_3.

The Effects of Rg_3 on the Activation and Inactivation of $Na_V1.2$. We next examined the effects of Rg_3 on the voltage-dependence of Na^+ channel steady-state activation and

inactivation. First, the effect of Rg_3 on Na^+ channel activation was determined by a conductance transformation of the peak current-voltage relationship (Fig. 3, A and B), with the curves representing the best data fit using the Boltzmann function. There was a significant depolarizing shift of the half-maximal activation voltage ($V_{g0.5}$). The $V_{g0.5}$ was -28.9 ± 0.57 mV in control experiments and -17.8 ± 0.21 mV in Rg_3-treated oocytes ($P < 0.01$, compared with control, $n = 10$). However, the slope factor (kg) was not significantly different, yielding values of 4.6 ± 0.5 mV under control conditions and 4.8 ± 0.2 mV after Rg_3 treatment. We then investigated the effect of Rg_3 on voltage-dependent Na^+ channel inactivation by plotting the normalized peak I_{Na} against the conditioning prepulse voltage (Fig. 3, C and D) and then fitting the data to the Boltzmann function. There was no significant difference in the half-maximal inactivation voltage ($V_{h0.5}$) and the slope factor (kh) between control and Rg_3 treatment groups; $V_{h0.5}$ was -28.9 ± 0.57 and -26.9 ± 0.68 mV, respectively, and kh was 7.2 ± 0.4 and 8.1 ± 0.68 mV, respectively ($n = 10$). These findings indicate that Rg_3 affects the steady-state activation but not inactivation of the Na^+ channel.

Use-Dependent Blockade of $Na_V1.2$ by Rg_3 and Lidocaine. Because Na^+ channel blockers such as lidocaine and other antiarrhythmic drugs exhibit use-dependent inhibition (Hondegham and Kazung, 1984), we tested whether Rg_3 behaved in the same way, using Rg_3 concentrations shown to induce minimal I_{Na} blockade (10 μM) and marked I_{Na} blockade (100 μM) in our initial tonic block experiments. I_{Na} was elicited by 20-ms pulses from -100 to -10 mV for 50 times at 10 Hz. Each peak I_{Na} was normalized to the first pulse peak I_{Na}. Under control conditions, there was a slight reduction in peak I_{Na}, whereas treatment with 10 and 100 μM Rg_3 induced use-dependent inhibitions of peak I_{Na} values by 11 ± 1 and $15 \pm 2\%$, respectively ($n = 9$ each; Fig. 4A). Lidocaine (1000 μM) treatment also induced a use-dependent inhibition

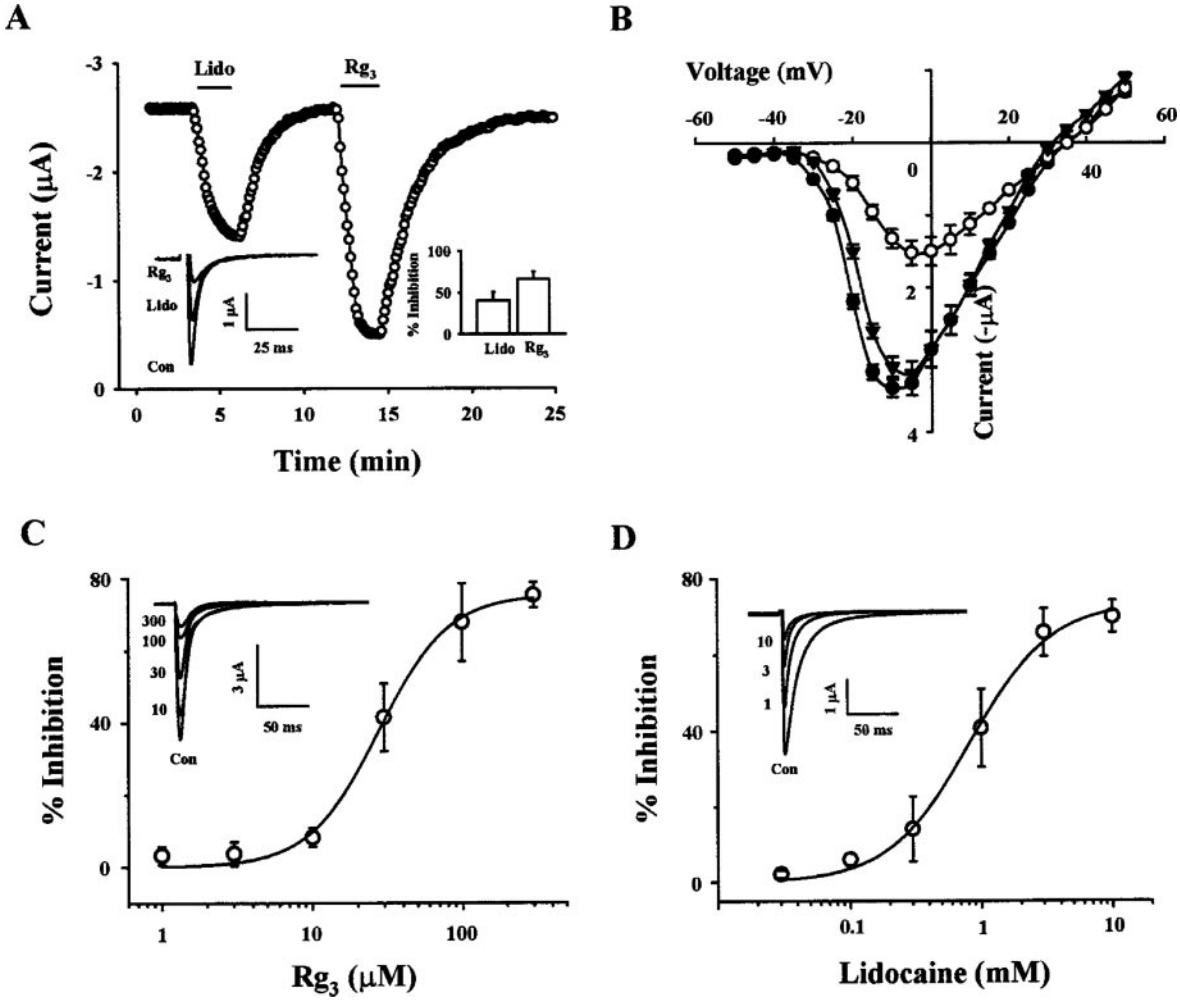

Fig. 2. Tonic inhibition of I_{Na} by Rg_3 and lidocaine. A, oocytes were injected with wild-type $Na_V1.2$ α and $\beta1$ subunit cRNAs and maintained for 2 to 4 days before Na^+ currents (I_{Na}) were recorded in ND96 using the two-electrode voltage clamp technique. ○, peak inward current amplitudes elicited by 100-ms depolarizations to -10 mV from a holding potential of -100 mV, evoked every 5 s. Rg_3 (100 μM) or lidocaine (1000 μM) were applied during the period indicated by the solid bars. Inset, left, traces are representatives of six separate oocytes from three different frogs. Inset, right, the histograms show the percentage blockade of peak I_{Na} by Rg_3 or lidocaine (Lido). Data represent the means ± S.E.M. (n = 10–13/group). B, the current-voltage relationship was obtained using voltage steps between -50 and $+50$ mV taken in 5-mV increments. Voltage steps were applied in the absence (●) and presence (○) of 100 μM Rg_3 or after washout of Rg_3 (▼). Data represent the means ± S.E.M. (n = 5–6/group). C and D, concentration-response curves for the Rg_3- (C) or lidocaine- (D) induced inhibition of peak I_{Na}. Inset, traces are representatives of six separate oocytes from three different frogs. The solid lines were fit by the Hill equation as described under *Experimental Procedures*. Data represent the means ± S.E.M. (n = 10–13/group).

of the peak I_{Na} by 35 ± 2% (n = 8 each) (Fig. 4A). Thus, Rg_3 and lidocaine both seemed to induce use-dependent inhibitions of I_{Na}.

The Effect of Rg_3 on Peak I_{Na} at Different Holding Potentials. The effect of Rg_3 on peak I_{Na} at different holding potentials was examined. Diphenylhydantoin (DPH), which is a well known anticonvulsant that preferentially binds to the inactivated Na^+ channel (Valenzuela et al., 1996), did not significantly affect the peak I_{Na} evoked at −10 mV from a holding potential of −110 mV (6 ± 1% inhibition by 100 μM, n = 10) (Fig. 5A). However, at a more depolarized holding potential of −50 mV, DPH dramatically reduced the peak I_{Na} (86 ± 7% inhibition by 100 μM, n = 10). This indicates that the blockade of peak I_{Na} by DPH is highly sensitive to the membrane potential and that DPH has a much higher affinity to the inactivated state than to the resting state of the Na^+ channel as shown by Kuo and Bean (1994) (Fig. 5, A and C, left). We then tested the effect of Rg_3 on the peak I_{Na} at different holding potentials. In contrast to the action of DPH, the inhibitory effect of 100 μM Rg_3 was not significantly affected by changes in the holding potential (78 ± 14% and 69 ± 10% inhibition at −110 and −50 mV, respectively; n = 15 each), indicating that the inhibitory effect of Rg_3 on the peak I_{Na} is independent of the membrane holding potential (Fig. 5, B and C, right).

Lidocaine and TTX Do Not Prevent Rg_3-Induced Inhibition of Peak I_{Na}. We performed occlusion experiments using lidocaine and TTX, which are well known Na^+ channel blockers, to determine whether Rg_3 shares a common binding site or pathway with lidocaine or TTX. As shown in Figs. 6B and D, single applications of 30 μM Rg_3, 1000 μM lidocaine and 1 nM TTX inhibited the peak I_{Na} values by 42 ± 8, 25 ± 5, and 44 ± 3%, respectively. Cotreatment of Rg_3 with lidocaine produced an additive inhibition of peak I_{Na} by 88 ± 4%, whereas cotreatment of Rg_3 with TTX produced an additive inhibition of peak I_{Na} by 80 ± 4%. These results suggest that Rg_3 regulates Na^+ channels by acting on different site(s) from those of lidocaine and TTX.

The Effect of Rg_3 on Mutant Na^+ Channels. To gain insight into the mechanism(s) by which Rg_3 inhibits peak

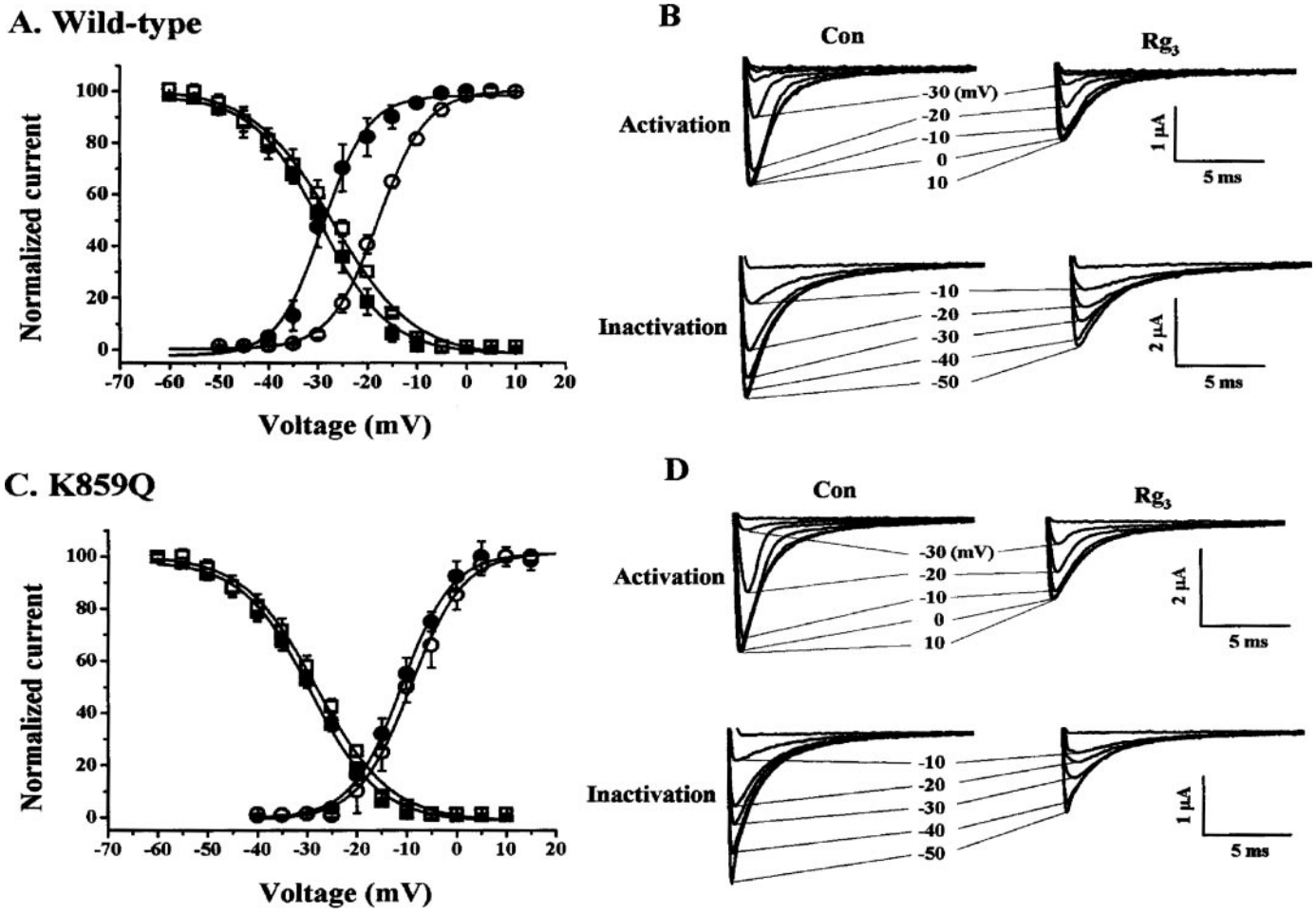

Fig. 3. The effect of Rg_3 on steady-state activation and inactivation of I_{Na} in wild-type and K859Q mutant channels. A, effect of Rg_3 on steady-state activation and inactivation of I_{Na} in wild-type channels. The voltage dependence of conductance was compared in the absence (●) and presence (○) of 100 μM Rg_3. Inactivation was measured using a two-pulse protocol in which oocytes were held at −100 mV and depolarized to potentials from −60 to +20 mV for 200 ms, followed by a test-pulse to −10 mV for 10 ms to determine channel availability. Inactivation curves are shown in the absence (■) and presence of 100 μM Rg_3 (□). B, representative current traces for the activation and inactivation of wild-type channels were obtained as described under *Experimental Procedures*. The indicated traces are presented for clarity. C, the effect of Rg_3 on the steady-state activation and inactivation of I_{Na} in the K859Q mutant. D, representative current traces for the activation and inactivation of the K859Q mutant channel were obtained as described. The indicated traces are represented for clarity. Data represent the means ± S.E.M. (n = 10–11/group). The curves represent a two-state Boltzmann function.

I_{Na}, we examined the requirement of different Na^+ channel α subunit protein domains using site-directed mutagenesis. We constructed the following six mutant types: 1) mutation of the channel pore entrance of the S6 segment of domain I by replacement of residue Tyr401 with cysteine (Y401C) or threonine (Y401T); 2) mutation at the channel pore sites by replacement of Glu942 with glutamine (E942Q), Glu945 with glutamine (E945Q), or Asp927 with asparagine (D927N) (Kontis and Goldin, 1993); 3) mutation of the lidocaine binding sites by replacement of residues Phe1764 and/or Tyr1771 with alanine (F1764A or Y1771A and F1764A-Y1771A, respectively) (Ragsdale et al., 1994; 1996); 4) mutation of the extracellular and intracellular TTX binding sites by replacement of Phe385 with cysteine (F385C), serine (F385S), tyrosine (F385Y), or methionine (F385M), or replacement F387 with glycine (F387G), threonine (F387T) or glutamine (F387Q) (Noda et al., 1989; Terlau et al., 1991); 5) mutation of the S4 voltage-sensor segments of domains I to IV by replacement of residues Lys226, Lys859, Arg1312, or Arg1638 with glutamine (K226Q, K859Q, R1312Q, or R1638Q) (Kontis et al., 1997); and 6) creation of a fast inactivation gating-deficient mutant (IFMQ3) (West et al., 1992). Representative traces were obtained from oocytes expressing channel pore, TTX binding site, and voltage-sensor mutants in the absence or presence of Rg_3 (Fig. 7A). Rg_3 treatment induced tonic inhibition of the peak I_{Na} in all mutants (Fig. 7 and Table 1). The concentration-response relationship for peak I_{Na} inhibition by Rg_3 in the different kinds of mutants was determined (Fig. 7B), and the data were fitted using the Hill equation. The Hill coefficients and V_{max} values for the mutants were not significantly different from those of the wild-type channels. However, the IC_{50} values from mutants F385M, E387Q, Y401C, and K859Q were significantly higher than that of the wild-type channel (*, $P < 0.01$ compared with wild-type channel) (Table 1). Because mutations of Phe1764 or Tyr1771 to alanine (F1764A or Y1771A) are resistant to lidocaine-induced tonic and use-dependent blockades (Ragsdale et al., 1994, 1996), we examined whether these mutations could affect the Rg_3-mediated tonic and use-dependent inhibitions of peak I_{Na}. Although lidocaine treatment induced only a slight inhibition of peak I_{Na} in oocytes expressing the F1764A, Y1771A, and F1764A-Y1771A mutants after low- and high-frequency stimulations (Fig. 8, A, C, and E, low-frequency stimulations; B, D, and F, high-frequency stimulations), Rg_3 treatment induced wild-type inhibition levels of peak I_{Na} in the mutants after in both low- and high-frequency stimulations (Fig. 8). The IFMQ3 mutant, which lacks fast inactivation, showed a slower decay and a sizable persistent noninactivating or plateau current at the end of a 500-ms depolarizing pulse to −10 mV in the absence of Rg_3, which is consistent with a previous report (West et al., 1992). In the IFMQ3 mutant, Rg_3 treatment induced dose-dependent inhibitions of peak and plateau I_{Na} (Fig. 9A). The plateau I_{Na} showed a larger change; the IC_{50} values of Rg_3 acting on the on peak and plateau I_{Na} in this mutant were 38 ± 3 and 14 ± 4 μM, respectively (approximately a 3-fold difference). These results suggest that Rg_3 interacts more readily with the open state of the Na^+ channel versus the resting state (Fig. 9B). Finally, we examined whether the IFMQ3 mutant showed any changes in the inhibitory effect of

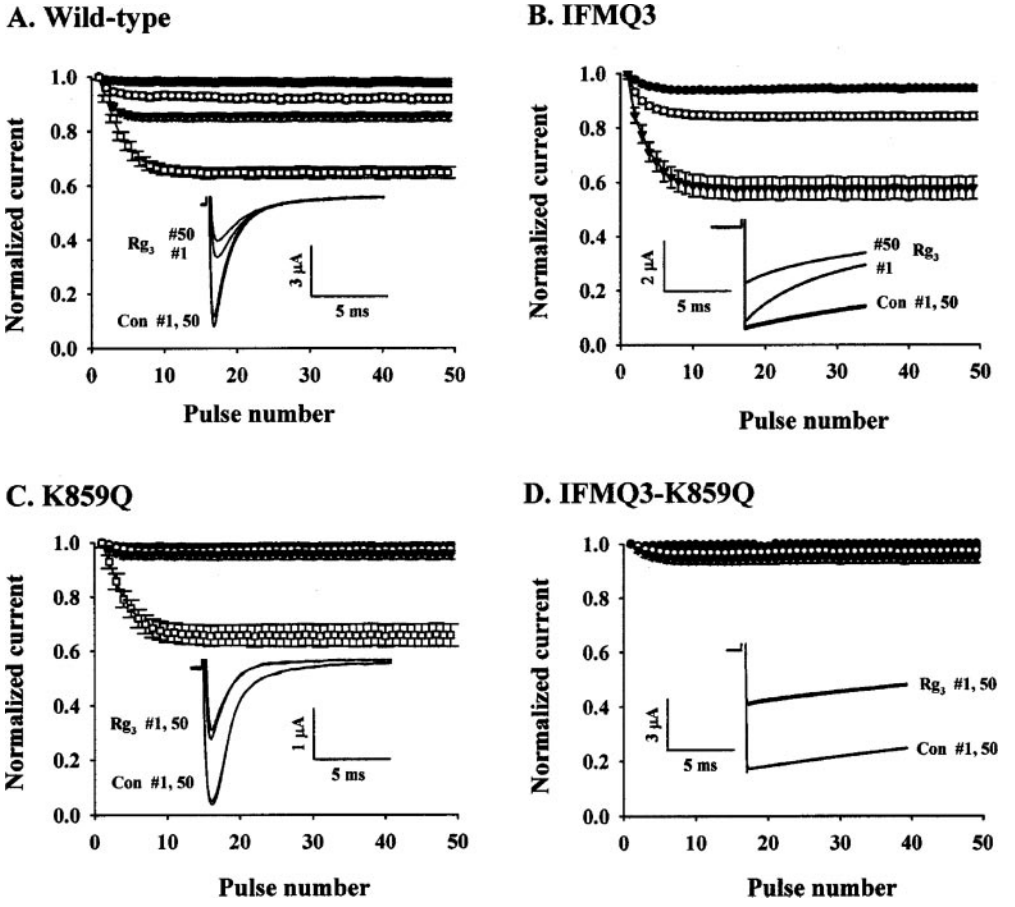

Fig. 4. Use-dependent block of Na^+ channels by Rg_3 or lidocaine. Fifty 20-ms depolarizing pulses to −10 mV were applied from a holding potential of −100 mV at 10 Hz in the absence (●) or presence of 10 μM (○) or 100 μM (▼) Rg_3 in wild-type (A), IFMQ3 (B), K859Q (C), and IFMQ3-K859Q (D) mutants. Lidocaine (1000 μM) (□) was also applied in wild-type (A) and the K859Q mutant (C). The current amplitude during each pulse was normalized to the peak current of the first pulse and plotted as a function of the pulse number. Inset, only sweeps 1 and 50 are shown for both control and Rg_3 treatment groups in the wild-type and mutants (IFMQ3, K859Q, and IFMQ3-K859Q). The other sweeps were omitted for clarity. Data represent the means ± S.E.M. (n = 9–10/group).

Rg_3 on oocytes subjected to high-frequency stimulation. We observed that Rg_3 treatment induced a 2- to 3-fold larger use-dependent inhibition in IFMQ3 mutant channels versus wild-type channels; 10 and 100 μM Rg_3 induced 17 ± 1 and 45 ± 4% use-dependent inhibitions of I_{Na}, respectively (n = 11) (Fig. 4, A and B). In contrast, Rg_3 did not induce additional use-dependent inhibitions in the other tested mutants (data not shown). Collectively, these results further demonstrate that Rg_3 uses different binding site(s) from those of lidocaine and TTX and that Rg_3 blocks the resting and open state of brain Na^+ channels.

A Point Mutation in the S4 Voltage-Sensor Segment of Domain II of $Na_V1.2$ Abolishes the Rg_3-Induced Voltage Shift of Na^+ Channel Activation. As shown in Fig. 3, A and B, Rg_3 treatment strongly depolarized the Na^+ channel activation voltage, suggesting that Rg_3 might modify its activation gating. The S4 segments comprise four homologous domains (I–IV) of the Na^+ channel and are believed to act as the voltage-sensing apparatus (Kontis et al., 1997). To investigate whether mutations in the voltage-sensor segments of the Na^+ channel affect the Rg_3-induced depolarization of the Na^+ channel activation voltage, we constructed four different mutants in the S4 segments of domain I to IV (Table 1) (Kontis et al., 1997) and examined their influences on the Rg_3-induced voltage shift of the Na^+ channel activation curve. Our results revealed that replacing Lys859 (domain II) with glutamine (K859Q) abolished the Rg_3-induced voltage shift, although the mutation itself resulted in a depolarizing shift of the activation curve by ~10 mV compared with wild-type channel (Fig. 3, C and D). The half-maximal activation voltage ($Vg_{0.5}$) was −10.9 ± 0.4 mV and the slope factor (kg) was 5.1 ± 0.3 mV in the Rg_3 control, but only −9.8 ± 0.4 mV and 5.3 ± 0.4 mV in the mutant (Fig. 3, C and D). The other tested mutants did not show significant alterations of the activation curve (data not shown), indicating that the Lys859 residue of domain II may play an important role in the Rg_3-induced modification of voltage-dependent Na^+ channel activation.

A Single Point Mutation in the S4 Voltage-Sensor Segment of Domain II of $Na_V1.2$ in Both Wild-Type and IFMQ3 Mutant Channels Abolishes Rg_3-Induced Use-Dependent Inhibition. We next examined whether the K859Q mutation affects the Rg_3-induced use-dependent inhibition of Na^+ channels, because this mutation abolished Rg_3-induced modification of Na^+ channel activation gating. Rg_3 treatment did not produce use-dependent inhibition in either K859Q or IFMQ3-K859Q mutants (Fig. 4, C and D), suggesting that the Lys859 residue of the S4 voltage sensor

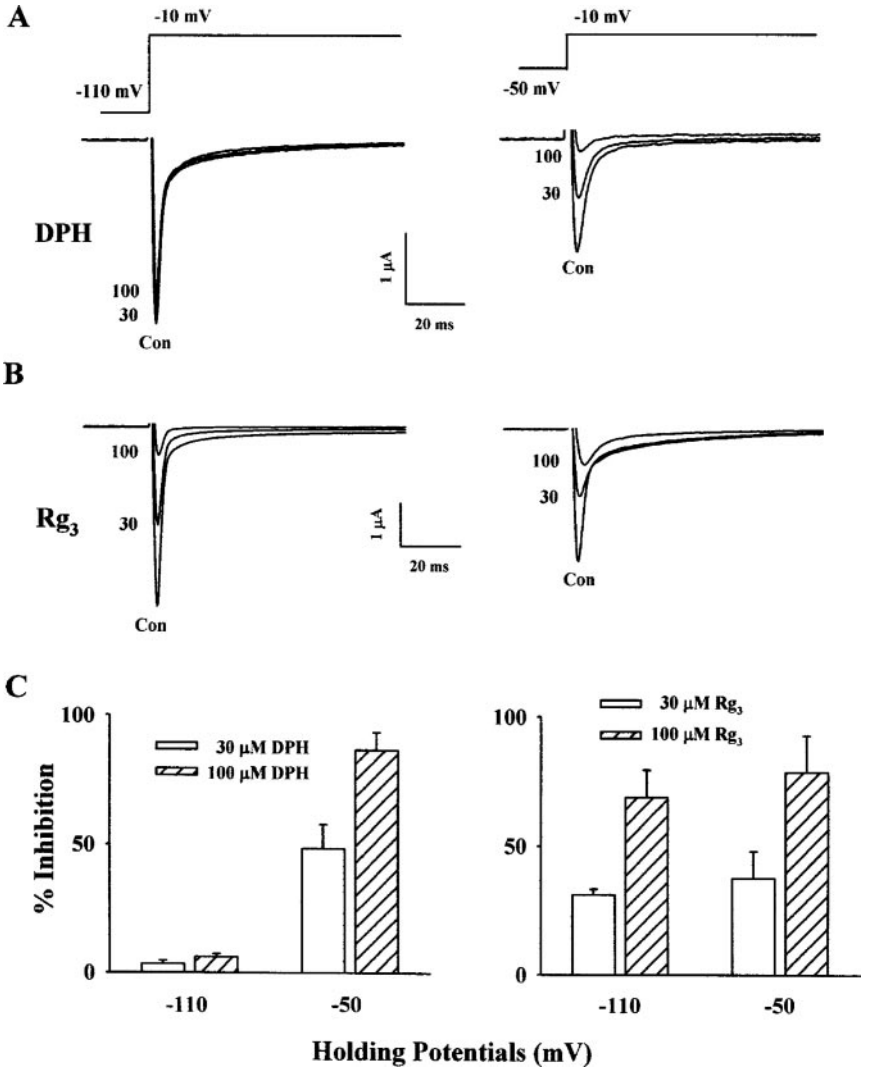

Fig. 5. Rg_3-induced I_{Na} inhibition is independent of the holding potential. A, representative traces of I_{Na} in the absence or presence of 30 or 100 μM phenytoin (DPH). Each oocyte was held at −50 or −100 mV and stepped to −10 mV for 100 ms every 5 s. B, representative traces of I_{Na} in control oocytes or those treated with 30 or 100 μM Rg_3. Each oocyte was held at −50 or −100 mV and stepped to −10 mV for 100 ms every 5 s. C, left, histograms for the inhibition of I_{Na} by 30 or 100 μM DPH at different holding potentials. C, right, histograms for the inhibition of I_{Na} by 30 or 100 μM Rg_3 at different holding potentials. Data represent the means ± S.E.M. (n = 10–11/group).

segment of domain II might play an important role in Rg_3-induced use-dependent inhibition of the IFMQ3 mutant. These mutations also significantly increased the IC_{50} values by 1.5-fold compared with wild-type in terms of tonic inhibition (*, $P < 0.01$, compared with wild-type; Table 1). It is noteworthy that lidocaine treatment produced wild-type level use-dependent inhibition in the K859Q mutant (Fig. 4C), suggesting that the Rg_3 site is not related with the action of lidocaine. In contrast, when we examined whether the mutation in the S4 voltage-sensor segment of domain II affected Rg_3-induced open-channel blocking pattern, we found that Rg_3 treatment inhibited both peak and plateau I_{Na} levels to comparable degrees in the IFMQ3-K859Q and IFMQ3 mutants (compare Fig. 9, C and A). The IC_{50} values of the IFMQ3-K859Q mutant were 56 ± 6 and 20 ± 1 μM for the peak and plateau I_{Na} levels, respectively (Fig. 9D and Table 1), which was significantly higher than that for the IFMQ3 mutant in terms of peak (1.5-fold) but not plateau I_{Na} inhibition (**, $P < 0.01$, compared with IFMQ3 mutant, Table 1). These results indicate that the K859Q mutant might decrease the affinity of Rg_3 for the IFMQ3 mutant to a comparable degree as that seen in the wild-type but that the K859Q mutation did not affect the Rg_3-induced open channel blocking pattern.

Developmental Rate of Rg_3-Induced Open Channel Blockade. We examined the ability of various concentrations of Rg_3 to block IFMQ3 (Fig. 10A). Untreated control traces showed that during a depolarizing pulse to −10 mV, the IMFQ3 current decayed exponentially with a single, slow time constant (τ_{slow}) of 585.4 ± 2.7 ms (n = 9). Currents elicited after Rg_3 treatment decayed exponentially with two distinct time constants. In the presence of low concentration of Rg_3 (10 μM), the currents decayed with a slow time constant that was similar to that of the control, whereas treatment with higher concentrations of Rg_3 such as 30 to 300 μM induced a concentration-dependent fast exponential component to the curves (τ_{fast}), which represented the Rg_3 block (τ_B). The time constants of the fast components were 464.5 ± 6.4, 235.1 ± 7.8, 64.1 ± 14.2, and 51.8 ± 9.4 ms in samples treated with 10, 30, 100, and 300 μM Rg_3, respectively. This result indicates that Rg_3 also interacts with the open state of the Na^+ channel. A plot of the reciprocal of τ_B ($1/\tau_B$) against drug concentration (Lansman et al., 1986) was used to approximate the drug-channel interaction kinetics. The relationship between $1/\tau_B$ and the concentration of Rg_3 was determined with a straight line representing the best fit to the equation $1/\tau_B = k_{on}[Rg_3] + l$. (Fig. 10B). The slope of the line is the apparent binding constant (k_{on}), which equals 0.062 ± 0.009 × 10^6 $M^{-1}s^{-1}$, and the intercept l equals 1.89 ± 0.78 s^{-1}. The latter value is close to the reciprocal of τ_{slow} (1.71 ± 0.41 s^{-1}), indicating that in the IFMQ3 mutant, a residual inactivation determines the intercept in the absence of Rg_3.

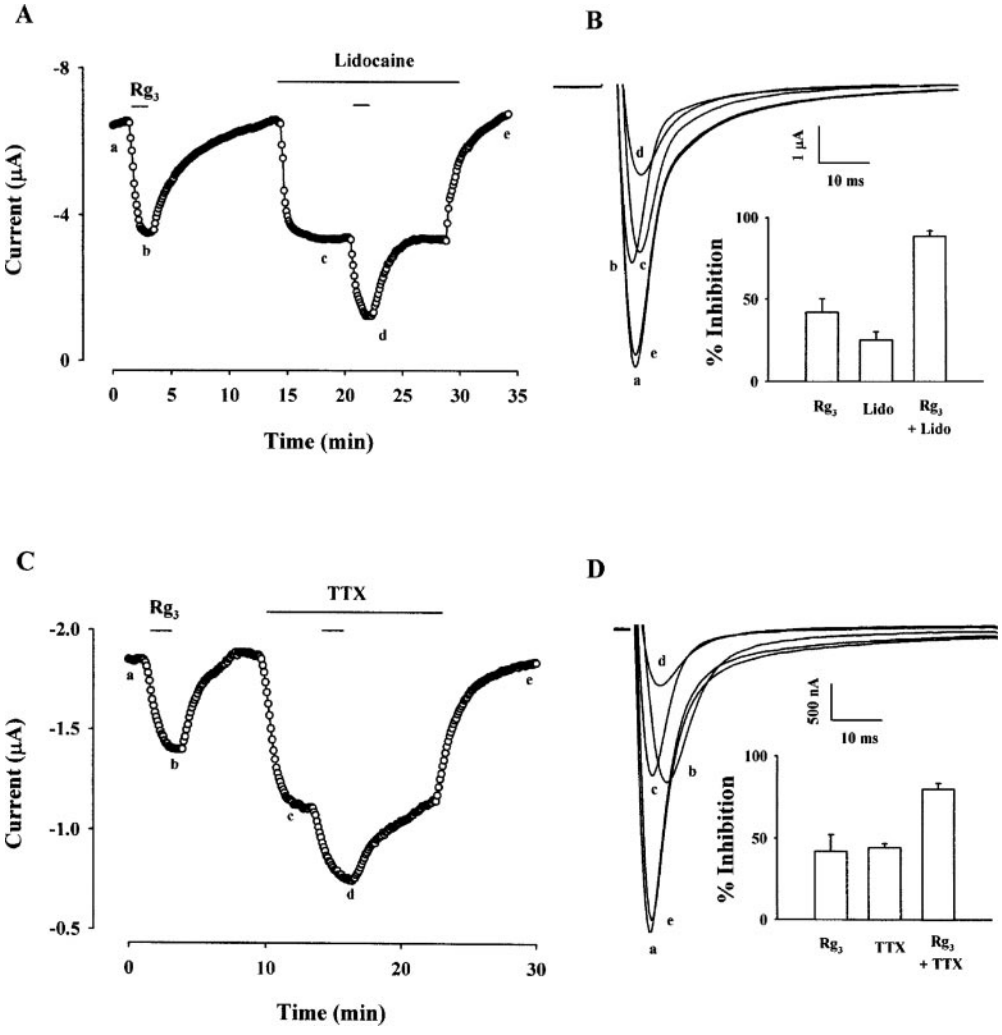

Fig. 6. Lidocaine and TTX do not interfere with the action of Rg_3. A, ○, peak inward current amplitudes elicited by 100-ms depolarizations to −10 mV from a holding potential of −100 mV, evoked every 5 s. Rg_3 (30 μM) was first applied during the period indicated by the solid bars, and then lidocaine (1000 μM) was applied in absence or presence of Rg_3 (30 μM) as indicated by the solid bars. B, traces are representatives of six separate oocytes from three different frogs. Inset, the histograms show the percentage blockade of I_{Na} by Rg_3, lidocaine (Lido), or Rg_3 + lidocaine (Lido). Data represent the means ± S.E.M. (n = 10–13/group). C and D, experiments were performed as above with TTX (1 nM) used in place of lidocaine. Data represent the means ± S.E.M. (n = 10–12/group).

This suggests that the unbinding constant (k_{off}) is likely to be very small.

Rg_3 Treatment Slows Recovery from Inactivation. Because Rg_3 blocked the open state of the IFMQ3 channel (Fig. 9) and exhibited an additional use-dependent block compared with the wild-type channel (Fig. 4B), we examined whether the inhibitory effect of Rg_3 on I_{Na} was derived from a delayed recovery of the channel from the open channel block. Current traces were recorded in the absence (Fig. 10C, control, top) and presence (Fig. 10C, bottom) of 100 μM Rg_3 with a recovery time interval of 10 ms between pulses. Recovery from open channel block was analyzed as shown in Fig. 10D. After a 10-ms prepulse (P1), recovery from open channel block was assessed using a test pulse (P2) after increasing recovery intervals (Fig. 10C and D, inset). The IFMQ3 Na^+ channels were found to recover rapidly, probably because of a slow inactivation associated with the mutation (Fig. 10D, $<$ 50 ms, ●). In contrast, Rg_3 treated channels (Fig. 10D, ○) showed a delayed recovery from open channel block (up to 260 ms). This slow recovery seems to underlie the enhanced use-dependent inhibition produced by Rg_3.

Discussion

Ginseng has long been used as a treatment for a wide variety of ailments, and some of the purported effects of this root have been documented in laboratory studies (Nah, 1997). Although the beneficial effects and functional mechanisms of ginsenosides have not been fully elucidated, accumulating evidence suggests that they may target the ion channels involved in neuronal excitability. Ginsenosides have been shown to affect several ion channels found at pre- and postsynaptic sites in the nervous system (Nah and McCleskey, 1994; Nah et al., 1995; Kim et al., 1998, 2002; Choi et al., 2002, 2003; Sala et al., 2002), and their effects are closely coupled to the inhibition of neurotransmitter release (Tachikawa et al., 1995; Kudo et al., 1998). We demonstrated recently that Rg_3 stereospecifically inhibits voltage-dependent brain Na^+ currents and that the carbohydrate portion of Rg_3 plays a key role in the inhibition of Na^+ currents (Kim et al., 2005). However, very little is known about the molecular mechanism(s) underlying Rg_3-induced Na^+ channel modulation.

Herein, we characterized Rg_3-induced channel regulation of brain Na^+ channels ($Na_V1.2$) expressed in *X. laevis* oocytes. Our results revealed four major findings. First, Rg_3 produced a tonic inhibition of the peak I_{Na} via an interaction with the resting state of the Na^+ channel (Fig. 2). Second, Rg_3 induced a large depolarizing shift in the steady-state activation of the Na^+ channel (Fig. 3). Third, Rg_3 produced a use-dependent block of the Na^+ channel after high-frequency stimulation, indicating that Rg_3 could exert an inhibitory effect on the open state of the Na^+ channel (Fig. 4). Fourth, the inhibitory effect of Rg_3 on the peak I_{Na} was independent of the holding potential, indicating that Rg_3 might have a

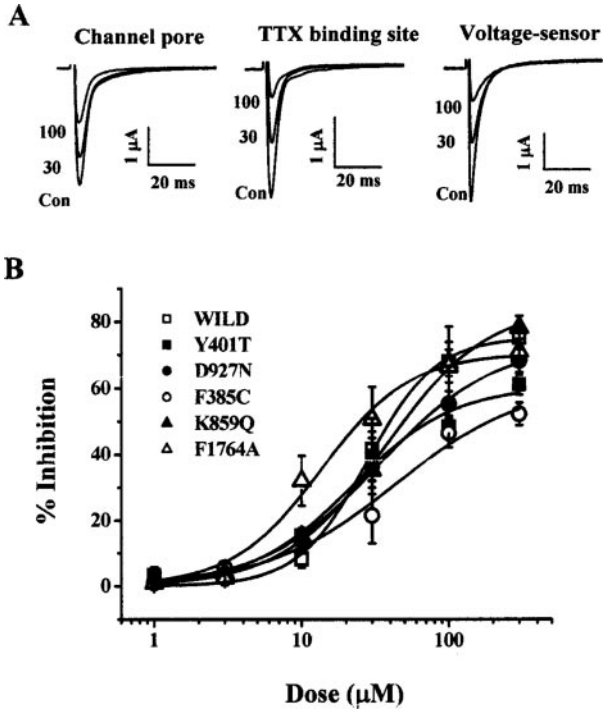

Fig. 7. Effect of Rg_3 on various mutant Na^+ channels. The site-directed mutants were generated at the channel pore, the lidocaine or TTX binding sites, and the S4 voltage sensor segment of domains I and II, as described under *Experimental Procedures*. A, traces are representative of six separate oocytes from three different frogs for analysis of channels with mutations in the channel pore, TTX interaction site, and S4 voltage sensor segment of domain II. B, representative concentration-response curves for the effect of Rg_3 on various mutants. The solid lines were fit by the Hill equation. Additional IC_{50}, Hill coefficient, and V_{max} values for the various mutants are presented in Table 1.

TABLE 1

Effect of Rg_3 on wild-type and various mutant Na^+ channels expressed in *X. laevis* oocytes

Data represent mean ± S.E.M. (n = 10–11/group). Currents were elicited by single-step voltage pulses from −100 to −10 mV at 0.2 Hz. The IC_{50}, Hill coefficient, and V_{max} values were determined as described under *Materials and Methods*.

Type	IC_{50}	n_H	V_{max}
Wild	32 ± 6	1.1 ± 0.4	75 ± 6
Pore entrance			
Y401C	43 ± 2*	1.5 ± 0.5	72 ± 2
Y401T	22 ± 5	1.3 ± 0.3	61 ± 5
Channel pore			
D927N	33 ± 4	1.1 ± 0.1	74 ± 3
E942Q	40 ± 9	1.3 ± 0.3	58 ± 6
E945Q	35 ± 5	1.2 ± 0.1	72 ± 4
Lidocaine binding site			
F1764A	23 ± 4	1.3 ± 0.4	71 ± 3
Y1771A	36 ± 6	1.1 ± 0.5	67 ± 5
F1764A-Y1771A	33 ± 5	1.2 ± 0.1	70 ± 3
TTX binding site			
F385C	26 ± 6	1.4 ± 0.4	52 ± 5
F385S	27 ± 3	1.4 ± 0.2	73 ± 3
F385Y	29 ± 9	1.2 ± 0.5	60 ± 9
F385T	26 ± 8	1.0 ± 0.5	67 ± 9
F385M	60 ± 6*	0.9 ± 0.4	84 ± 3
E387G	36 ± 4	1.2 ± 0.1	85 ± 3
E387T	29 ± 2	1.3 ± 0.4	60 ± 2
E387Q	44 ± 9*	1.1 ± 0.2	75 ± 6
Voltage sensor			
Domain I K226Q	30 ± 3	1.4 ± 0.2	65 ± 3
Domain II K859Q	47 ± 9*	1.1 ± 0.1	88 ± 7
Domain III R1312Q	30 ± 2	1.2 ± 0.7	73 ± 2
Domain IV R1638Q	33 ± 6	1.0 ± 0.7	62 ± 3
Inactivation site			
IFMQ3			
Peak	38 ± 3	1.1 ± 0.1	70 ± 5
Plateau	14 ± 4	1.3 ± 0.4	98 ± 1
IFMQ3-K859Q			
Peak	56 ± 6**	1.1 ± 0.3	76 ± 6
Plateau	20 ± 1	1.4 ± 0.3	97 ± 2

* $P < 0.01$ compared with wild-type Na^+ channel.
** $P < 0.01$ compared with IFMQ3 mutant.

lower affinity for the inactivated state of the Na^+ channel (Fig. 5).

To examine the molecular mechanism by which Rg_3 regulates brain Na^+ channel activity, we used site-directed mutagenic methods similar to those previously used to identify drug- or toxin-Na^+ channel interaction site(s) (Cestele and Catterall, 2000). We used six different types of $Na_V1.2$ mutants to assess the sites at which Rg_3 interacts with Na^+ channels: 1) mutations in the channel pore entrance of the S6 segment of domain I; 2) mutations in the pore region of domain II; 3) mutations in the lidocaine binding sites; 4) mutations in the TTX binding sites; 5) mutations in the S4 voltage-sensor segments of domains I, II, III, and IV; and 6) mutations in the inactivation cluster. The pore site(s) are unlikely to be the target for Rg_3, because the inhibitory potency of Rg_3 on Na^+ channel activity was not altered in cells injected with pore site mutants (Fig. 7 and Table 1). In addition, it does not seem as though Rg_3 interacts with the binding sites for lidocaine or TTX (Ragsdale et al., 1994, 1996), because the inhibitory potency of Rg_3 on Na^+ channel activity was not altered in cells injected with the F385C, F385S, F385Y, F385T, F385M, E387G, E387T, E387Q, F1764A, Y1771A, or F1764A-Y1771A mutants, which harbor changes in the lidocaine or TTX binding sites (Fig. 7 and Table 1). In addition, the inhibitory effect of Rg_3 on the peak I_{Na} seemed additive in the presence of lidocaine or TTX in

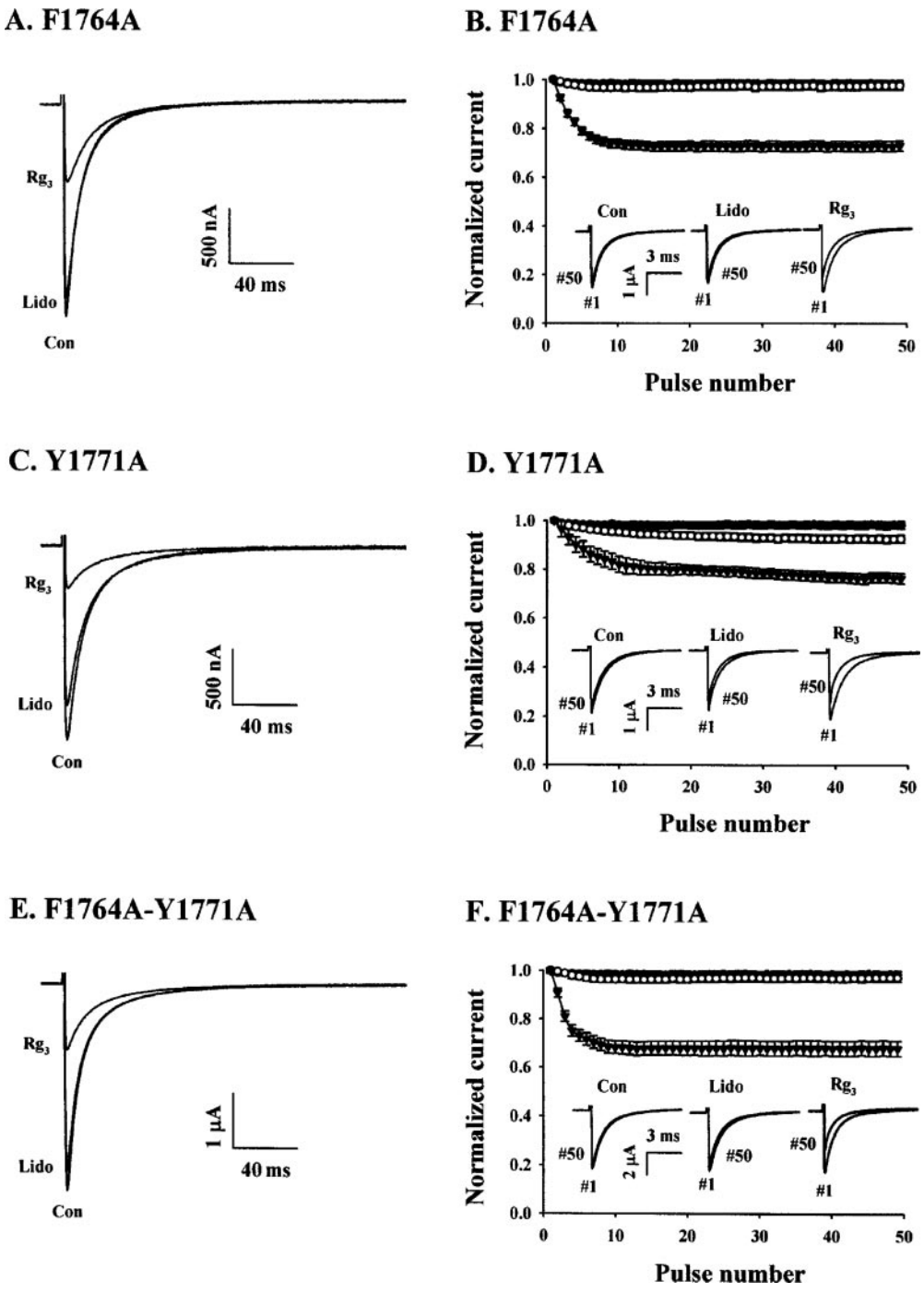

Fig. 8. The effect of Rg_3 or lidocaine on F1764A, Y1771A, and F1764A-Y1771A mutant Na^+ channels. The site-directed mutants F1764A, Y1771A, and F1764A-Y1771A were constructed as described under *Experimental Procedures*. A, C, and E, traces are representatives of six separate oocytes from three different frogs for the F1764A (A), Y1771A (C), and F1764A-Y1771A (E) mutants, respectively. B, D, and F, Rg_3 but not lidocaine inhibited peak I_{Na} in a use-dependent manner in the F1764A (B), Y1771A (D), and F1764A-Y1771A (F) mutants. Insets, only sweeps 1 and 50 are shown for control (●), 1000 μM lidocaine (○), and 100 μM Rg_3 (▼). The other sweeps were omitted for clarity. Data represent the means ± S.E.M. (n = 9–10/group).

occlusion experiments (Fig. 6, C and D), providing further evidence that Rg_3 uses a separate binding site. Finally, we tested the possibility that the hydrophobic cluster related with Na^+ channel inactivation might be involved in the Rg_3-induced inhibition of I_{Na}. In the IFMQ3 mutant channel, which lacks fast inactivation (West et al., 1992), Rg_3 treatment inhibited the noninactivating plateau I_{Na} to a greater degree than the peak I_{Na}, providing further evidences that Rg_3 inhibits I_{Na} in both the open and resting states of the Na^+ channel.

Two other lines of evidence that support the possibility that Rg_3 also inhibits open Na^+ channels are the observations that 1) the inhibitory effect of Rg_3 on peak I_{Na} is not dependent on membrane holding potentials and 2) Rg_3 does not shift the steady-state inactivation curve in wild-type Na^+ channels (Figs. 3 and 5), which does occur in many drugs (e.g., antiarrhythmic agents and anticonvulsants) that act on inactivated Na^+ channels (Willow et al., 1985). Moreover, Rg_3 treatment induced an additional use-dependent block of I_{Na} in the IFMQ3 mutant compared with wild-type channel, indicating that Rg_3 might prefer to bind and block the open state of the Na^+ channel. Similar use-dependent open channel blockades have been observed in the case of disopyramide, RSD921, tetracaine, and flecainide (Cahalan, 1978; Grant et al., 1996; Pugsley and Goldin, 1999; Wang et al., 2003; Ramos and O'Leary, 2004).

We next used S4 voltage-sensor segment mutants (K226Q, K859Q, R1312Q, and R1368Q) to examine whether the voltage-sensor segment of the Na^+ channel was involved in Rg_3-induced Na^+ channel regulation (Noda et al., 1989). The K859Q mutation in domain II, but not K226Q, R1312Q, or R1638Q, significantly increased the IC_{50} values by 1.5-fold compared with wild-type (*, $P < 0.01$, compared with wild-type; Table 1), indicating that this mutation might decrease the affinity of Rg_3 to Na^+ channels. In addition, K859Q alone abolished the Rg_3-induced voltage shift in Na^+ channel activation (Fig. 3C) and Rg_3-induced use-dependent but not tonic inhibition of I_{Na} (Figs. 4C and 7). Although these results do not allow precise elucidation of the interaction between Rg_3 and Na^+ channels, our data seem to indicate that the voltage-sensor S4 segment of domain II might be an important portion for Rg_3-induced Na^+ channel regulation (Figs. 3C and 4C). It is unlikely that Rg_3 interacts nonspecifically with Na^+ channels, because the 20(*S*)-ginsenoside Rg_3 used in the present study inhibits I_{Na} but 20(*R*)-ginsenoside Rg_3 does not (Jeong et al., 2004) (Fig. 1). Moreover, modifications of the hydrophilic portion of Rg_3 by opening the cyclic glucoses or conjugating the glucoses with other hydrophobic molecule abolished the inhibitory effect of Rg_3 on peak I_{Na} (Kim et al., 2005). These findings indicate that Rg_3 specifically modulates Na^+ channel by interaction with unidentified site of Na^+ channel. Further works will be necessary to determine specific interaction site(s) of Rg_3 with Na^+ channel.

Based on our findings, it seems reasonable to speculate as

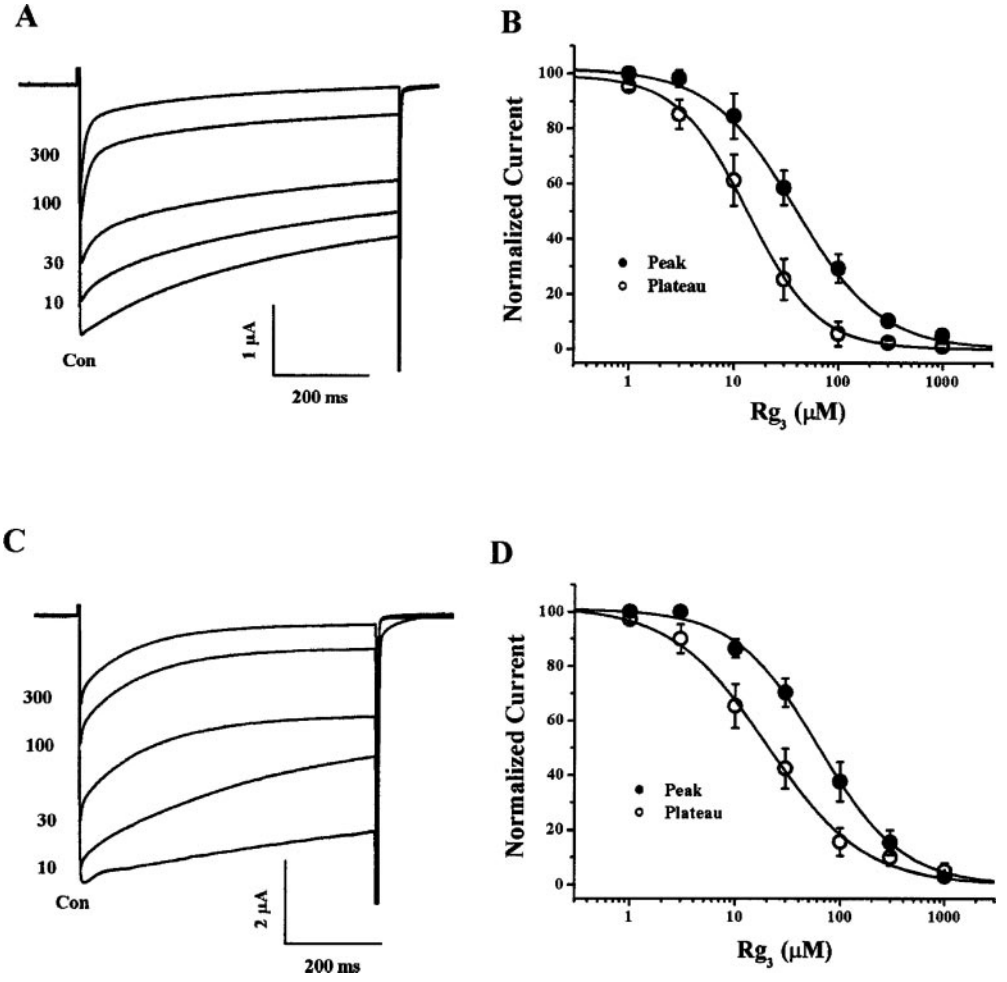

Fig. 9. The effects of Rg_3 on IFMQ3 mutant Na^+ channels. The IFMQ3 mutant was constructed as described under *Experimental Procedures*. A, I_{Na} was elicited in IFMQ3 mutant by a 500-ms depolarization to −10 mV from a holding potential of −100 mV, evoked every 5 s. The evoked current exhibited a slower decay and sizable persistent noninactivating or plateau current. Rg_3 treatment dose dependently inhibited the peak and plateau I_{Na} values. B, concentration-response curves for the effect of Rg_3 on the IFMQ3 peak (●) and plateau (○) I_{Na} values. The solid lines were fit by the Hill equation. C, current traces of the IFMQ3-K859Q mutant in the absence or presence of Rg_3 were obtained from the procedures described in A. D, concentration-response curves for the effect of Rg_3 on IFMQ3-K859Q peak (●) and plateau (○) I_{Na} values. The IC_{50}, Hill coefficient, and V_{max} values for Rg_3 in these mutants are presented in Table 1. Data represent the means ± S.E.M. (n = 10–11/group).

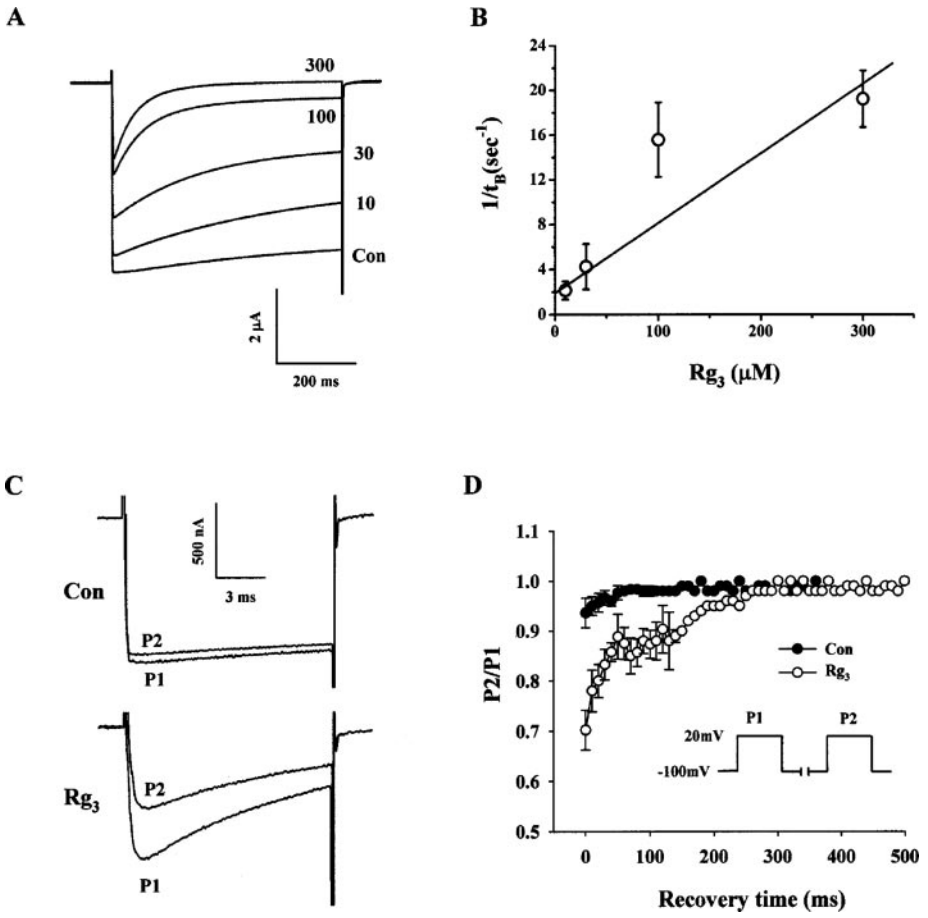

Fig. 10. Kinetics of open channel blockade by Rg_3 and recovery delay in IFMQ3 mutant Na^+ channels. A, traces evoked from −100 mV to −10 mV in the absence (Con) and presence of various concentrations of Rg_3 showing open channel blockade of IFMQ3. B, the rate of Rg_3 block as a function of Rg_3 concentration. A detailed description of the determination of t_B can be found in the text. Data represent the means ± S.E.M. (n = 10–12/group). C, delayed recovery of IFMQ3 channels from open channel blockade by Rg_3. Shown is a representative pair of current traces recorded in the absence (Con, top) and presence (Rg_3, bottom) of 100 μM Rg_3 with a recovery time interval of 10 ms between pulses. Channels recovered almost fully at this recovery interval in the absence of Rg_3. In the presence of 100 μM Rg_3, the test current measured during the second pulse (P2) was significantly reduced. D, recovery from inactivation or open channel blockade was assessed in detail using the paired-pulse voltage-clamp protocol shown in the inset. After oocytes were depolarized for 10 ms (P1), fractional recovery during a subsequent test pulse (P2) was assessed after an intervening recovery interval. Rg_3 (●)-free channels recovered rapidly (<50 ms), whereas complete recovery from inactivation was delayed for 260 ms in the presence of Rg_3 (○). Data represent the means ± S.E.M. (n = 9–10/group).

to whether the in vitro Rg_3-induced Na^+ channel blockade could translate to in vivo pharmacological effects. Qian et al. (2005) and Xie et al. (2005) determined plasma concentration of Rg_3 after administration of Rg_3 via intravenous (5 mg/kg) or intragastric (10 mg/kg) routes in rats and found that plasma Rg_3 peaked at 1 μg/ml 10 min after intravenous administration and 4 h after intragastric administration. These findings suggest that plasma-borne Rg_3 might exert in vivo pharmacological effects. In addition, in rats, Bae et al. (2004) and Tian et al. (2005) showed that oral (100 mg/kg) or intravenous administration (5 and 10 mg/kg) of Rg_3 exerted significant neuroprotective effects against focal cerebral ischemic injury by decreasing neurological deficit scores and reducing the infarct area compared with the control group. Rg_3 also significantly improved mitochondrial energy metabolism, antagonized decreases in superoxide dismutase and glutathione-peroxidase activities, and increased malondialdehyde levels in a cerebral ischemia model (Tian et al., 2005). Na^+ channel-blocking drugs such as local anesthetics, antiarrhythmics, and anticonvulsants have been shown to exhibit significant neuroprotective effects against cerebral ischemia-, hypoxia-, and head trauma-induced neuronal damages (Taylor and Meldrum, 1995). Thus, it is possible that Rg_3-mediated brain I_{Na} inhibition could be an underlying mechanism for neuroprotection against in vivo ischemic brain injury.

We demonstrated previously that Rg_3 and other ginsenosides inhibit voltage-dependent Ca^{2+} and K^+ channels as well as ligand-gated ion channels such as 5-HT_3 and some subsets of nicotinic acetylcholine receptors (Nah et al., 1995; Choi et al., 2002, 2003; Jeong et al., 2004). We are currently examining the detailed characteristics of Rg_3-mediated regulation of Ca^{2+}, K^+, and ligand-gated ion channels. The elucidation of the regulatory modes and identification of interaction site(s) with those channels or receptors by Rg_3 and other ginsenosides will provide important insights into the molecular basis by which ginsenosides interact with membrane proteins such as ion channels and receptors.

In this study, we used brain Na^+ channel gene expression in a *X. laevis* oocyte model system to show that Rg_3 blocks the resting and open state of brain Na^+ channels. This novel work provides new insights into one possible mechanism underlying the effects of ginsenosides in the nervous system.

References

Bae EA, Hyun YJ, Choo MK, Oh JK, Ryu JH, and Kim DH (2004) Protective effect of fermented red ginseng on a transient focal ischemic rats. *Arch Pharm Res (Seoul)* **27:**1136–1140.

Bean BP, Cohen CJ, and Tsien RW (1983) Lidocaine block of cardiac sodium channels. *J Gen Physiol* **81:**613–642.

Cahalan MD (1978) Local anesthetic block of sodium channels in normal and pronase-treated squid giant axons. *Biophys J* **23:**285–311.

Catterall WA (1987) Identification of an alpha subunit of dihydropyridine-sensitive brain calcium channels. *Trends Pharmacol Sci* **8:**57–65.

Cestele S and Catterall WA (2000) Molecular mechanisms of neurotoxin action on voltage-gated sodium channels. *Biochime* **82:**883–892.

Choi S, Jung SY, Lee JH, Sala F, Criado M, Mulet J, Valor LM, Sala S, Engel AG, and Nah SY (2002) Effects of ginsenosides, active components of ginseng, on nicotinic acetylcholine receptors expressed in Xenopus oocytes. *Eur J Pharmacol* **442:**37–45.

Choi S, Lee JH, Oh S, Rhim H, Lee SM, and Nah SY (2003) Effects of ginsenoside Rg_2 on the 5-HT_{3A} receptor-mediated ion current in *Xenopus* oocytes. *Mol Cells* **15:**108–113.

Dascal N (1987) The use of Xenopus oocytes for the study of ion channels. *CRC Crit Rev Biochem* **22:**317–387.

Goldin AL (1995) Voltage-gated Na^+ channels, in *Ligand- and Voltage-Gated Ion Channels* (North RA ed), pp 73–89, CRC Press, Boca Raton, FL.

Grant AO, John JE, Nesterenko VV, Starmer CF, and Moorman JR (1996) The role of inactivation in open-channel block of the sodium channel: studies with inactivation-deficient mutant channels. *Mol Pharmacol* **50:**1643–1650.

Hodgkin AL and Huxley AF (1952) A quantitative description of membrane current and its application to conduction and excitation in nerve. *J Physiol (Lond)* **117:** 500–544.

Hondegham LM and Kazung BG (1984) Antiarrhythmic agents: the modulated receptor mechanism of action of sodium and calcium channel-blocking drugs *Annu Rev Pharmacol Toxicol* 24:387–423.

Jeong SM, Lee JH, Kim JH, Lee BH, Yoon IS, Lee JH, Kim DH, Rhim H, Kim Y, and Nah SY (2004) Stereospecificity of ginsenoside Rg_3 action on ion channels. *Mol Cells* **18:**383–389.

Kim HS, Lee JH, Goo YS, and Nah SY (1998) Effects of ginsenosides on Ca^{2+} channels and membrane capacitance in rat adrenal chromaffin cells. *Brain Res Bull* **46:**245–251.

Kim JH, Hong YH, Lee JH, Kim DH, Jeong SM, Lee BH, Lee SM, and Nah SY (2005) A role for the carbohydrate portion of ginsenoside Rg_3 in Na^+ channel inhibition. *Mol Cells* **19:**137–142.

Kim S, Ahn K, Oh TH, Nah SY, and Rhim H (2002) Inhibitory effect of ginsenosides on NMDA receptor-mediated signals in rat hippocampal neurons. *Biochem Biophysical Res Comm* **296:**247–254.

Kontis KJ and Goldin AL (1993) Site-directed mutagenesis of the putative pore region of the rat IIA sodium channel. *Mol Pharmaocol* **43:**635–644.

Kontis KJ, Rounaghi R, and Goldin AL (1997) Sodium channel activation gating is affected by substitutions of voltage sensor positive charges in all four domains. *J Gen Physiol* **110:**391–401.

Kudo K, Tachikawa E, Kashimoto T, and Takahashi E (1998) Properties of ginseng saponin inhibition of catecholamine secretion in bovine adrenal chromaffin cells. *Eur J Pharmacol* **341:**139–144.

Kuo CC and Bean BP (1994) Slow binding of phenytoin to inactivated sodium channels in rat hippocampal neurons. *Mol Pharmacol* **46:**716–725.

Lansman JB, Hess P, and Tsien RW (1986) Blockade of current through single calcium channels by Cd^{2+}, Mg^{2+} and Ca^{2+}. Voltage and concentration dependence of calcium entry into the pore. *J Gen Physiol* **88:**321–347.

Nah SY and McCleskey EW (1994) Ginseng root extract inhibits calcium channels in rat sensory neurons through a similar path, but different receptor, as μ-type opioids. *J Ethnopharmacol* **42:**45–51.

Nah SY, Park HJ, and McCleskey EW (1995) A trace component of ginseng that inhibits Ca^{2+} channels through a pertussis toxin-sensitive G protein. *Proc Natl Acad Sci USA* **92:**8739–8743.

Nah SY (1997) Ginseng, recent advances and trend. *Korea J Ginseng Sci* **21:**1–12.

Noda M, Suzuki H, Numa S, and Stühmer W (1989) A single point mutation confers tetrodotoxin and saxitoxin insensitivity on the sodium channel II. *FEBS Lett* **259:**213–216.

Pugsley MK and Goldin AL (1998) Effects of bisaramil, a novel class I antiarrhythmic agent, on heart, skeletal muscle and brain Na^+ channels. *Eur J Pharmacol* **343:**93–104.

Pugsley MK and Goldin AL (1999) Molecular analysis of the Na^+ channel blocking actions of the novel class I anti-arrhythmic agent RSD 921. *Br J Pharmacol* **127:**9–18.

Pugsley MK, Yu EJ, and Goldin AL (2000) Spiradoline, a kappa opioid receptor agonist, produces tonic- and use-dependent block of sodium channels expressed in Xenopus oocytes. *Gen Pharmacol* **34:**417–427.

Qian T, Cai Z, Wong RN, Mak NK, and Jiang ZH (2005) In vivo rat metabolism and pharmacokinetic studies of ginsenoside Rg_3. *J Chromatogr B Analyt Technol Biomed Life Sci* **816:**223–232.

Ragsdale DS, McPhee JC, Scheuer T, and Catterall WA (1994) Molecular determinants of state-dependent block of Na^+ channels by local anesthetics. *Science (Wash DC)* **265:**1724–1728.

Ragsdale DS, McPhee JC, Scheuer T, and Catterall WA (1996) Common molecular determinants of local anesthetic, antiarrhythmic and anticonvulsant block of voltage-gated Na^+ channels. *Proc Natl Acad Sci USA* **93:**9270–9275.

Ramos E and O'Leary ME (2004) State-dependent trapping of flecainide in the cardiac sodium channel. *J Physiol* **560:**37–49.

Sala F, Mulet J, Choi S, Jung SY, Nah SY, Rhim H, Valor LM, Criado M, and Sala S (2002) Effects of ginsenoside Rg_2 on human neuronal nicotinic acetylcholine receptors. *J Pharmacol Exp Ther* **301:**1052–1059.

Stuart GJ and Sakmann B (1994) Active propagation of somatic action potentials into neocortical pyramidal cell dendrites. *Nature (Lond)* **367:**60–72.

Tachikawa E, Kudo K, Kashimoto T, and Takahashi E (1995) Ginseng saponins reduce acetylcholine-evoked Na^+ influx and catecholamine secretion in bovine adrenal chromaffin cells. *J Pharmacol Exp Ther* **273:**629–636.

Taylor CP and Meldrum BS (1995) Na^+ channels as targets for neuroprotective drugs. *Trends Pharmacol* **16:**309–316.

Terlau H, Heinemann SH, Stühmer W, Pusch M, Conti F, Imoto K, and Numa S (1991) Mapping the site of block by tetrodotoxin and saxitoxin of sodium channel II. *FEBS Lett* **293:**93–96.

Tian J, Fu F, Geng M, Jiang Y, Yang J, Jiang W, Wang C, and Liu K (2005) Neuroprotective effect of 20(S)-ginsenoside Rg_3 on cerebral ischemia in rats. *Neurosci Lett* **374:**92–97.

Valenzuela C, Delpon E, Franqueza L, Gay P, Perez O, Tamargo J, and Snyders DJ (1996) Class III antiarrhythmic effects of zatebradine. Time-, state-, use- and voltage-dependent block of hKv1.5 channels. *Circulation* **94:**562–570.

Wang GK, Russell C, and Wang SY (2003) State-dependent block of wild-type and inactivation-deficient Na^+ channels by flecainide. *J Gen Physiol* **122:**365–374.

West JW, Patton DE, Scheuer T, Wang Y, Goldin AL, and Catterall WA (1992) A cluster of hydrophobic amino acid residues required for fast Na^+ channel inactivation. *Proc Natl Acad Sci USA* **89:**10910–10914.

Willow M, Gonoi T, and Catterall WA (1985) Voltage clamp analysis of the inhibitory actions of diphenylhydantoin and carbamazepine on voltage-sensitive sodium channels in neuroblastoma cells. *Mol Pharmacol* **27:**549–558.

Xie HT, Wang GJ, Sun JG, Tucker I, Zhao XC, Xie YY, Li H, Jiang XL, Wang R, Xu MJ, et al. (2005) High performance liquid chromatographic-mass spectrometric determination of ginsenoside Rg_3 and its metabolites in rat plasma using solid-phase extraction for pharmacokinetic studies. *J Chromatogr B Analyt Technol Biomed Life Sci* **818:**167–173.

Address correspondence to: Prof. Seung-Yeol Nah, Research Laboratory for the Study of Ginseng Signal Transduction and Dept. of Physiology, College of Veterinary Medicine, Konkuk University, Seoul 143-701, Korea. E-mail: synah@konkuk.ac.kr